Sample containment for neutron and high-energy x-ray scattering studies of hydrogen fluoride and related molecular species

ARTICLE *in* REVIEW OF SCIENTIFIC INSTRUMENTS · OCTOBER 2003

Impact Factor: 1.61 · DOI: 10.1063/1.1611999

Sample containment for neutron and high-energy x-ray scattering studies of hydrogen fluoride and related molecular species

John F. C. Turner[a)]
Neutron Sciences Consortium and Department of Chemistry, University of Tennessee, Knoxville, Tennessee 37996-1600

Sylvia E. McLain
Department of Chemistry, University of Tennessee, Knoxville, Tennessee 37996-1600 and Intense Pulsed Neutron Source, Argonne National Laboratory, 9700 S. Cass Avenue, Argonne, Illinois 60439

Timothy H. Free
Department of Chemistry, University of Tennessee, Knoxville, Tennessee 37996-1600

Chris J. Benmore
Intense Pulsed Neutron Source, Argonne National Laboratory, 9700 S. Cass Avenue, Argonne, Illinois 60439

Kenneth W. Herwig
Spallation Neutron Source, Oak Ridge National Laboratory, 701 Scarboro Road, Oak Ridge, Tennessee 37830

Joan E. Siewenie
Intense Pulsed Neutron Source, Argonne National Laboratory, 9700 S. Cass Avenue, Argonne, Illinois 60439

(Received 17 April 2003; accepted 28 July 2003)

The design of a suite of sample cells and sample preparation facilities to investigate the structure and dynamics of chemically reactive molecular fluorides, using high-energy x-ray and neutron scattering, is reported. A detailed discussion of both the neutronic and chemical considerations is provided, in support of the choice of the material of cell construction for both structural and dynamical experiments. The discussion of this suite of equipment also includes a detailed design of a hybrid high-vacuum Schlenk line for sample preparation. These cells were specifically designed to study hydrogen fluoride but may be used for other species that exhibit similar chemical reactivity. Background considerations for liquid diffraction experiments are also discussed and show that in designing cells for liquid samples, or samples that contain a large structurally amorphous fraction, crystalline sample containment affords far more tractable data analysis. © *2003 American Institute of Physics.* [DOI: 10.1063/1.1611999]

I. INTRODUCTION

Fluoride-based materials are among some of the most interesting systems available and display a wide range of structural, chemical, and bonding properties which lead to their application both in industry,[1–4] synthesis,[5,6] and in more fundamental, academic studies.[7,8]

Fluorine, as a ligand to both transition metals and main group elements is unique in the range of high oxidation states that it will support. The thermodynamic reason for this lies in part in the bond energy of the F–F bond,[9–11] which is low in comparison to the other halogens[11,12] [$D_0(F_2) = 158.78\ \mathrm{kJ\,mol^{-1}}; D_0(Cl_2) = 242.58\ \mathrm{kJ\,mol^{-1}}; D_0(Br_2) = 192.807\ \mathrm{kJ\,mol^{-1}}; D_0(I_2) = 151.088\ \mathrm{kJ\,mol^{-1}}$] and, also, in the strength of the heteroatomic bonds formed in a reaction with fluorine, which are almost always strong. The small steric encumbrance of the F atom also ensures that fluorine is a very strong π donor; in transition metal chemistry, it is a weak field ligand, consistent with strong π donation under the molecular orbital and ligand field theory of transition metal chemistry.[13] These electronic and thermodynamic properties ensure that the properties of fluoride complexes of an element are often anomalous when compared to the general trends of the chemistry of that element. The best examples of this are to be found in the chemistry of the noble gases. Indeed, it was oxidation of Xe by PtF_6 (Refs. 14 and 15) that opened up an entirely new group in the Periodic Table to chemical discovery, a chemical event not witnessed since the isolation of the alkali and alkaline earth metals by Davy. Examples of the unique structures and bonding motifs are to be found in the respective structures of O_2F_2,[16] XeF_6,[17–20] and F_2H^-.[21,22] Moreover, fluorinated inorganic fluids, such as HF, $HF.SbF_5$, FSO_3H, and $FSO_3H.SbF_5$ are the strongest acids known and are highly important fluids both academically and industrially.[5–7] Recent work into the structure of superacids and superacidic solutions[23–25] using neutron diffraction from liquid samples has required the development of appropriate sample environment (SE) equipment.

In order to apply neutron scattering and high-energy x-ray scattering to chemically ambitious samples, SE equipment that satisfies the chemical and experimental constraints must be designed and built. The work reported in this article contributes to this effort, and indeed, recent advances in SE

a)Author to whom correspondence should be addressed; electronic mail: jturner@atom.chem.utk.edu

equipment have lead to the development of facilities to study chemical reactions *in situ* or in a time-resolved manner.[26–28] These include the hydrothermal crystallization of dense phase materials and zeolites,[29–32] chemical reactions,[26] and catalytic processes.[27,28] In this article, the design, construction, and preliminary results using a suite of handling apparatus and sample cells are reported which allow the measurement of structural and dynamical properties of highly aggressive and reactive samples with the conservation of both chemical and isotopic integrity. Specifically, the experimental development involved in the measurement of the dynamics and structure of isotopomers of anhydrous liquid hydrogen fluoride is described. Hydrofluoric acid is an exceptionally dangerous material to handle; it has a very high chemical toxicity and causes severe and highly dangerous burns in contact with human tissue, even in aqueous solution.[33,34] Anhydrous hydrogen fluoride is even more dangerous due to the high fat solubility and volatility. In the design of the equipment, the chemical containment must, therefore, meet very severe safety constraints.

This article also demonstrates that the stringent constraints of the neutronic properties of hydrogen, of the interplay between sample structure and the structure of the material used in cell construction and those of the chemical nature of the sample can be satisfied and that neutron and high-energy x-ray scattering can be applied to chemically difficult samples.

Current fluences[35] and new instruments[36,37] recently built at neutron sources and third-generation x-ray sources[38] have significantly widened the range and complexity of chemical samples for which these types of scattering can provide detailed structural and dynamical information. The projected increase in flux at the Spallation Neutron Source,[39] presently under construction, will only amplify this trend. With respect to neutron scattering, this is a highly desirable development; neutron scattering is a particularly attractive technique chemically as the method is highly sensitivity to light atoms, defined as those with a low atomic number. This sensitivity is general for elastic neutron scattering experiments and is true for quasielastic and inelastic neutron scattering spectroscopy in a more qualified manner.

Information from elastic neutron scattering experiments is often complementary to that from the x-ray scattering analog. The complementary nature of the two techniques is due to the differing nature of the neutron-matter and x-ray-matter interaction;[40,41] elastic neutron scattering reveals the distribution of nuclear density (or magnetic spin density in certain cases) in the sample whereas the scattering density in an x-ray scattering experiment is the distribution of the electron density. Particularly well known is the sensitivity of elastic neutron scattering to hydrogen and deuterium but in general across the Periodic Table, atoms with low atomic number scatter as strongly as those with high atomic number,[42,43] in direct contrast with x rays, where the scattering power increases with the atomic number.[44] Inelastic and quasielastic experiments are extraordinarily sensitive to normal modes that involve the motion of protons in the system whether the protons are bound chemically or are translationally free. In contrast to vibrational or rotational spectroscopies, such as infrared or microwave spectroscopies, or Raman scattering, there are in general no selection rules that govern the existence of a normal mode transition.

These features of elastic, inelastic, and quasielastic neutron scattering are, in themselves, highly desirable; this desirability is only amplified by the complementary nature of the data from a neutron scattering experiment to that collected from x-ray and electromagnetic spectroscopies.

High-energy synchrotron x-ray diffraction, and its precursor γ-ray scattering, shares many of the features of neutron scattering in terms of the level of penetration possible in condensed matter.[45,46] Recently, this technique has begun to be applied to the investigation of electron density distributions[47–50] and quantum effects on the structure of liquids.[45,47–49,51–55]

II. DESIGN CONSTRAINTS

A. Neutronic considerations

Although the interaction between the nucleus and the neutron is very strong, the low density of nuclear matter in a material of average density ensures that the net interaction of neutrons with matter is extremely weak. Coupled with the lack of charge on the neutron, this gives neutron scattering one of its major experimental advantages—that of great penetration. Not only does this mean that structures and dynamics measured by neutron scattering are genuine representations of the structural and dynamical characteristics of the thermodynamic state of the sample, but also that the range of materials out of which SE equipment can be built is wider than that for analogous experiments with x rays of conventional energies. The penetration of neutrons is such that almost any nonabsorbing material may be used, allowing the construction of high-temperature and high-pressure apparatus that would be impossible at an x-ray source. An exception to this generality is the use of diamond anvil cells in x-ray diffraction experiments; such cells are only now being developed for work at neutron sources. That diamond anvil cells can be used easily in x-ray experiment is a feature of the large discrepancy in the fluences at current neutron and x-ray sources. Sample sizes for x-ray experiments need often be much smaller than at a neutron source.

The range of physical variables that is, therefore, accessible to neutron scattering investigation is often wider than the analogous x-ray experiment. The caveat to this lack of proscription of construction material is that the background, which the cell material presents in the scattering experiment, must be accounted for in the data analysis and ideally considered beforehand in the design of the SE equipment.

By paying careful attention to the neutronic properties of the elements of which the apparatus is constructed, several unique approaches to sample environment design are available. Neutronically, vanadium or alloys, such as $Ti_{2.08}Zr$, are common materials for construction of SE equipment for neutron scattering experiments, due to the mechanical and neutronic properties of the metals. Vanadium and $Ti_{2.08}Zr$ are chosen because of the elastic scattering cross sections these materials possess. The former has a very small elastic cross section ($b_V = -0.3824$ fm) (Refs. 42 and 43) and is pre-

dominately an incoherent scatterer, while the latter exploits the opposite phase of the scattered neutrons when scattered from Ti or Zr, which is denoted by a negative length for Ti ($b_{Ti}=-3.438$ fm; $b_{Zr}=7.16$ fm).[42,43] As long as the Ti and Zr atoms reside on the same site in the alloy, a cell constructed from $Ti_{2.08}Zr$ has no coherent elastic cross section and as such, presents no elastic background.

However, Ti, Zr, and V are chemically reactive, and, being electropositive, are especially susceptible to oxidation. They are suitable for conventional chemical samples but not for acidic, protic, or oxidizing samples,[56–59] where the chemical stability of these elements is low and the sample may corrode or weaken the cells with potentially unpleasant results. Given the possibility of neutron activation with certain materials, the hazards are also not purely chemical. The material from which the SE equipment is constructed requires a balance between safely containing hazardous, reactive samples and minimizing the scattering background.

B. Chemical considerations

There are several commercially available materials which can safely contain fluoride-containing samples, among them polytetrafluoroethylene (PTFE) and alloy 400 ($Ni_{1.86}Cu$).[60] Of these, PTFE has the greater general resistant to fluorides at low temperatures and pressures, especially in the presence of traces of water. Copper and nickel are also both largely resistant to attack by fluorides and can be treated with F_2 to passivate the surface through the formation of a fluoride surface coating which renders these materials resistant to further attack.[61] Indeed, Alloy 400 and nickel are used as the material of choice in the construction of many high valent fluorides. Consequently, the construction outlined below should be applicable to any fluoride that is stable in Alloy 400 or nickel. For materials that contain hydronium ions, such as aqueous solutions of HF and FSO_3H, this containment is probably not suitable. The constraint of chemical resistance is required in experiments such as these in order to preserve both the chemical and isotopic purity of the sample, as well as for radiological considerations.

C. Elastic background scattering considerations

PTFE is a partially crystalline material[62–64] and the phase diagram is known.[65,66] The diffraction pattern from this material, which forms the background, contains Bragg peaks, which arise from the periodic crystalline lattice, together with a diffuse component which arises from the local and intermediate range atomic correlations. There also exists a phase transition in PTFE that occurs at 303 K, which is an added factor in any consideration of the background signal.

Alloy 400 is a polycrystalline material, the scatter from which is predominately Bragg in nature, with low levels of diffuse scatter. Figure 1(a) shows the diffraction pattern recorded on the glass, liquids, and amorphous materials diffractometer (GLAD) at the Intense Pulsed Neutron Source;[67] Fig. 1(b) shows the corresponding pair distribution function for both materials. The high-energy x-ray data would produce a similar pattern, differing only in regard to peak intensities and is, therefore, not shown.

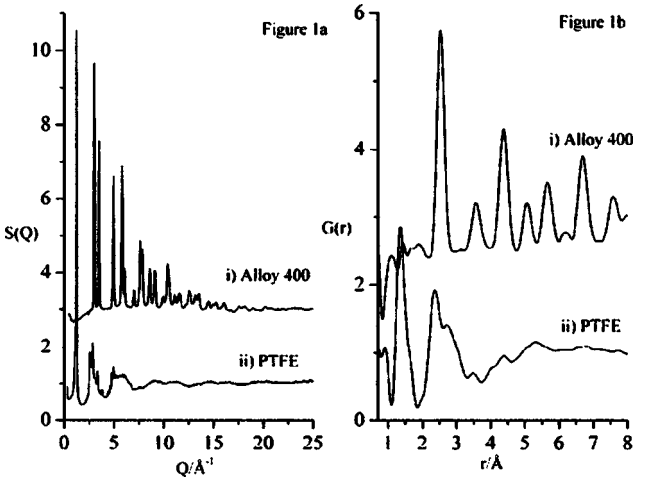

FIG. 1. (a) Diffraction pattern of (i) alloy 400 $[(S(Q)+2]$ and (ii) PTFE $[(S(Q)]$. (b) Fourier transformation of the diffraction pattern of (i) alloy 400 $[(G(r)+3]$ and (ii) PTFE $[(G(r)]$.

The samples, for which this suite of SE equipment was designed, were liquids and as such, exhibit a complete absence of Bragg scatter, due to the absence of any lattice; the diffraction intensity is confined to diffuse scatter. The choice of material is, therefore, crucial if the subtraction of background signal is to be successful. In the subtraction of a diffuse background from diffuse sample scatter, there is no simple *a priori* method for determining from what source the diffuse signal is recorded—sample or cell. In this respect, the material most suitable for sample containment in a liquid diffraction experiment of this type is alloy 400, even though Cu and Ni both have a large neutron scattering cross section ($b_{Ni}=10.3$ fm), ($b_{Cu}=7.718$ fm),[42,43] and therefore have Bragg peaks of very large intensity. However, subtraction of the prominent Bragg intensity is possible, both through standard analysis procedures[45,68] and through empirical subtraction.

D. Attenuation and multiple scattering considerations

When running neutron diffraction experiments on samples containing a large amount of hydrogen it is necessary to reduce the thickness of the sample in the beam since the high incoherent scattering cross section of hydrogen ($\sigma_{incoh}=80.3$ b) leads to large multiple scattering effects. Even a 1-mm-thick sample of HF has a significant multiple scattering contribution of ~20% and an absorption coefficient of ~5% neglecting the container at $2\theta=20°$ and 1.8 Å. Therefore, a flat plate geometry is optimal as it maximizes the number of atoms in the beam while minimizing the multiple scattering.[69] In comparison for a 6.6-mm-thick flat plate DF sample the total scattering cross section is 5.82 b/atom yielding multiple scattering contribution of ~15% and an absorption coefficient of only ~2% at $2\theta=20°$ and 1.8 Å. The low absorption and respectable coherent scattering cross section of DF allows relatively large samples to be placed in the beam without significant attenuation or multiple scattering effects. Considerations for the HF sample thickness in high-energy x-ray experiments (~115 keV) are also based on the minimization of multiple scattering and attenuation ef-

fects. It has been found that while the multiple scattering effects have a significant Q dependence, the attenuation coefficient is usually relatively constant with momentum transfer at high energies.[70] However, it is expected that these effects will show a greater angular dependence for a flat plate geometry sample, than for a cylindrical one. For a 115 keV incident x-ray beam the calculated attenuation coefficient (obtained using the method described by Soper *et al.*)[71] from a 4 mm HF sample is approximately 6% and the multiple scattering contribution only ~2%. The multiple Bragg scattering and attenuation due to the heavy elements in the alloy 400 container are far greater than that from the HF sample. However, since the sample is small and is comprised of light elements, the single and multiple scattering effects from the metal container do not differ significantly with or without the presence of a sample.

In order to minimize multiple scattering in inelastic and quasielastic experiments, the total scattering strength of the sample including the sample cell is typically restricted to ensure 90%–92% total transmission.[72] In the case of HF, the macroscopic cross-section is approximately 2.7 cm^{-1} at the elastic energy of the spectrometer, ~4.3 meV ($\sigma^{HF}_{incoh} \times \rho_{HF} = 90\ b \times 0.03$ H atoms/$Å^3$). For a 92% transmission, this results in an ideal sample thickness along the beam direction of 0.3 mm. The sample cell will provide a relatively strong, additional signal centered at zero energy transfer.

III. SAMPLE CELL DESIGN FOR STRUCTURAL AND DYNAMICAL MEASUREMENTS OF HYDROGEN FLUORIDE

A. Diffraction cells

All parts of the diffraction cells with the exception of the valves and the ''o'' rings are machined from alloy 400. They all consist of two separable parts; a cell head which allows for transfer of hydrogen fluoride via the vacuum line described below and a sample cell body in which the sample is contained during the diffraction experiment. The two parts are joined using a 1 in. SwageLok® nut and a PTFE o-ring seal. The sample cells constructed for the diffraction experiments are shown in Fig. 2.

The body of the sample cell head was machined from alloy 400 bar stock. In order to load the samples into the body of the cell the top portion of the cell head was drilled with a 6.35 mm bore that turns 90° in approximately the middle of the head. A piece of 6.35 mm OD alloy 400 seamless tubing was welded onto the outside top of the cell in order to connect the needle valve. The lower portion of the head was additionally machined with threads to fit a SwageLok® 1 in. nut, which allows for the connection with the body of the sample cells. At this interface, a knife edge was machined to present a sealing surface to the o-ring. Appropriately sized PTFE o-rings were machined to effect the vacuum seal.

In order to minimize background container scattering, the wall thickness of each cell body was machined as thin as possible, while still maintaining the integrity of the container. The composition of the sample and the type of radiation used constrained the cell body design further. It is necessary to have a cell body of sufficient length so that only sample and the thinnest part of the can encounter the radiation beam while keeping cell head from adding to further background contamination.

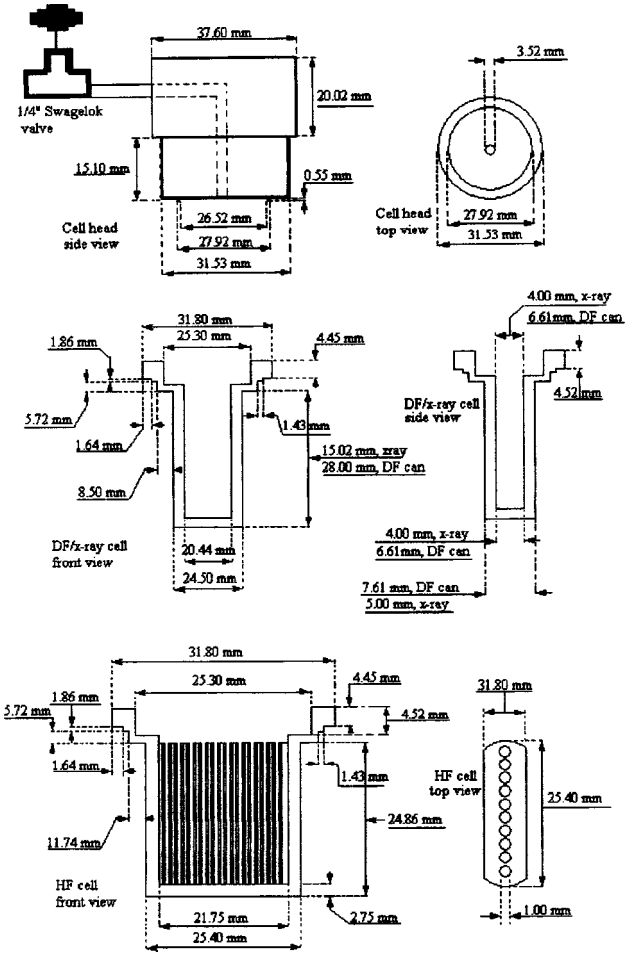

FIG. 2. Neutron and high energy x-ray diffraction sample cells.

The design and dimensions of the x-ray and DF neutron cells are shown in Fig. 2. In the case of all of the x-ray samples and the deuterium fluoride neutron sample, the cell bodies were machined as large as possible within the wall thickness, multiple scattering, and attenuation constraints. This allowed for a 6.60 mm sample thickness in the case of the deuterium fluoride neutron measurement and a 4 mm sample in thickness in the high-energy x-ray experiments. The hydrogen fluoride neutron cell body was of a different design (Fig. 2) this cell was constructed by soldering individual pieces of alloy 400 tubing (1.5 mm OD, 1 mm ID) to an alloy 400 frame using Safety-Silv® 45% silver cadmium free silver solder in a Stay-silv® black high temperature flux.

B. Quasielastic cells

In a quasielastic experiment, which utilizes the incoherent scatter from hydrogen, the sample cell has a limited volume to minimize the large signal from hydrogen. The cell body and cell heads (Fig. 3) are of a similar construction to the diffraction cells where the two portions can be joined by a Swagelok® $\frac{1}{2}$ in. nut. The cell head is of the same design as

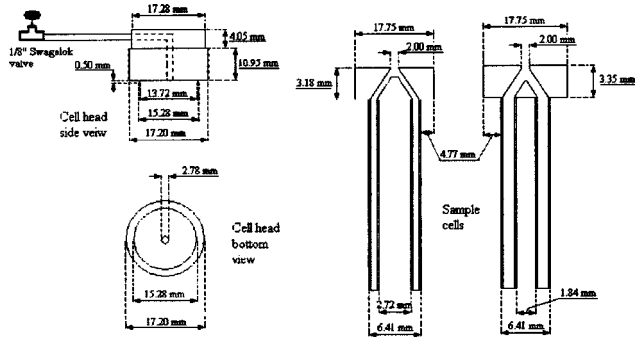

FIG. 3. Quasielastic cells.

the diffraction cell heads (Fig. 2) but on a smaller scale, with the bore in the cell being 3.14 mm.

Because the of the small sample size thickness ($\sim$0.3 mm for HF and $\sim$1.9 mm for $H_{0.04}D_{0.96}F$), the cell bodies were fabricated from available alloy 400 seamless tubing, to form an appropriately sized annulus. In each case a 6.41 mm OD$\times$4.93 mm ID tube was used for the outer portion of the annulus and smaller sized tubing was used to give the appropriate sample thickness. In the case of HF, the inner tube was 4.76 mm OD and in the case of $H_{0.04}D_{0.96}F$, the inner tube was 3.18 mm OD. For each set of samples the thickness was somewhat less than ideal, but the calculation ignored the scattering from the seamless alloy 400 tubing. In order to effectively vacuum transfer the samples into the cell bodies, a split Y bore was drilled into the top of the cell body to allow for access to the annulus created by the tubing. The tubing was welded to the top of the cell body by the same method described above.

IV. DESIGN OF THE SYNTHESIS AND GAS HANDLING APPARATUS

The neutron and x-ray experiments for which these cells were designed required the preparation of isotopomers of hydrogen fluoride of known composition. Not only must the chemical purity of the sample be retained at all times, but also the isotopic nature of the samples needed to be similarly conserved. Given the lability in reaction of the H/D site in anhydrous hydrogen fluoride, ingress of water and other proton-containing materials had to be minimized. The basic techniques for satisfying these requirements are mature in the field of inorganic chemistry.[61]

In order to prepare and handle hydrogen fluoride and deuterium fluoride in the laboratory, both synthetically and in order to prepare samples for the neutron experiments, a high vacuum line was constructed from alloy 400 and stainless steel tubing and equipped with SwageLok® fittings and needle valves. As a further precaution against contamination, and to allow the manipulation of liquids via Schlenk methodologies, an argon gas line was incorporated into the design. The synthetic equipment is therefore a hybrid Schlenk–high-vacuum line and is hereafter termed the gas handling line.

The gas handling line consists of five major components: vacuum, argon, fluorine, and hydrogen fluoride circuits, connected to a central manifold.

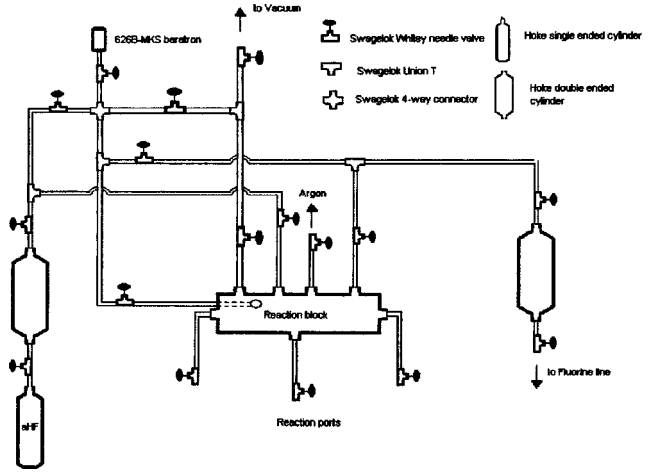

FIG. 4. Reaction manifold for the high-vacuum line.

A. Manifold design

The 214.2 mm$\times$51 mm$\times$51 mm manifold is machined from alloy 400 bar stock. A 37.8 mm diameter bore is drilled into the center of the manifold and finished as closely as possible to a mirror finish to minimize any adsorption of gas and potential reactivity problems on passivation. The ports are drilled and then tapped with NPT connections; the NPT connections are sealed using Teflon tape. The manifold is shown in Fig. 4. Prior to assembly, the manifold was closely examined for burr and any residual imperfections were removed, for the same reasons as the finishing of the interior bore. A port to the low pressure MKS 626A Baratron allows the pressure in the manifold to be measured.

B. F_2 and hydrogen fluoride circuits

The fluorine circuit (Fig. 5) and hydrogen fluoride circuit (Fig. 4) are constructed from 6.35 mm OD (4.57 mm ID) seamless alloy 400 tubing and are equipped with Swagelok® $\frac{1}{4}$ in. alloy 400 or 316 stainless steel needle valves. In order to provide a large constant volume, 2000 ml Hoke® bottles, constructed from 316 stainless steel, are introduced in the circuit. The fluorine circuit is additionally equipped with a

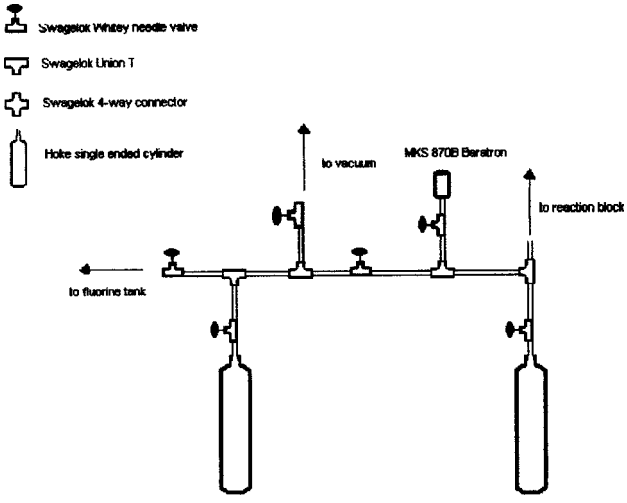

FIG. 5. Fluorine circuit.

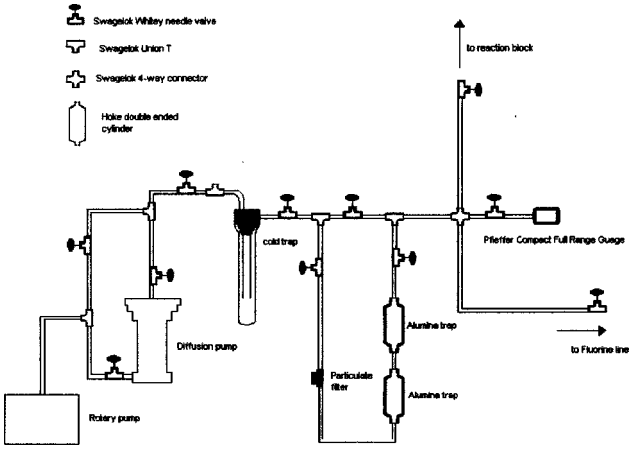

FIG. 6. Vacuum circuit.

higher pressure (1000 psi) MKS 870B baratron for measurement of higher pressures of fluorine than the manifold baratron will allow.

C. Vacuum circuit

The vacuum line (Fig. 6) is constructed entirely from 12.7 mm OD, 10.9 mm ID 316 stainless steel seamless (SS) tubing and is equipped with SwageLok® $\frac{1}{2}$ in. 316 stainless steel needle valves. There are two traps in place on the system. The first contains pelletized Al_2O_3, used as a scrubber trap for fluorine; the second trap is a removable glass liquid nitrogen cryogenic trap for the removal of volatiles before the pump, attached to a 316 SS trap head and sealed with Apiezon® W black wax. The scrubber can be bypassed for faster pumping and is fitted with a sintered steel 320 μm particulate filter down stream. The scrubber can also be removed and recharged without interruption of the line function.

The vacuum system is connected to the manifold (Fig. 4) and to the fluorine system (Fig. 5). The line is evacuated using a diffusion pump with Fomblin® as the working fluid, with a two-stage rotary pump as a roughing pump, the latter using conventional hydrocarbon pump oil. The diffusion pump is fitted with a bypass valve to allow for evacuation using only the roughing pump.

Pressure measurement was conducted using two electronic manometers, with ranges of 0–1000 Torr and 0–1000 psi (1 Torr = 0.001 333 bar; 1 psi = 0.068 948 bar), respectively. The magnitude of the vacuum was measured using a combination Pfieffer Pirani–cold cathode ion gauge, with a range of $0-10^{-8}$ mbar. All wetted parts of the gauges were constructed from Inconel®.

V. CONSTRUCTION OF THE SYNTHESIS AND GAS HANDLING APPARATUS

Before commencing with assembly and use, all tubing was thoroughly degreased using ''gum solvent,'' a mixture by volume of 1:1:1 toluene:acetone:methanol until evaporation of the solvent left no visible residue. The tubing and other components were then freed of traces of solvent and other oxidizable volatiles by fast passage of O_2 and the line was then assembled, according to the designs described above.

The line was then both vacuum leak-tested and pressure tested with Ar. All portions of the line, except the vacuum line, were volume calibrated with Ar repeatedly, so that each segment can be used as a constant volume, allowing the barometric measurement of molar quantities of gas. It was found to maintain a static vacuum of 10^{-5} mbar over a period of weeks. After leak testing and calibration, and in order to pre-dry the line prior to drying and passivation with F_2, the line was evacuated and dried by heating the system strongly under high vacuum.

Passivation is an important aspect of the construction of any fluorine line and the portions of the gas handling line that would be wetted by F_2 or hydrogen fluoride were passivated initially by evacuation and then pressurization at ambient temperatures to sub-ambient pressures with a 5% solution of F_2 in N_2. After any pressure drop had ceased, the line was evacuated and the procedure was repeated at slightly higher initial pressure. Once atmospheric pressure had been attained and no further decrease in pressure was observed, the cycle of pressurization and evacuation was repeated with F_2 until atmospheric pressure had been reached. A pressure of 1.5 bar of F_2 was then admitted and the line left under this pressure for 24 h. Finally, the line was evacuated.

Reaction vessels and synthesis bombs are attached to the outlets from the manifold and volatiles are transferred by standard cryogenic techniques.

VI. DISCUSSION

Neutron diffraction experiments performed on samples of DF, HF, and $H_{0.5}D_{0.5}F$, prepared using the above equipment and cells showed that the conservation of the isotopic nature of the samples was essentially that of the materials used to prepare the samples and that no measurable ingression of adventitious [H] occurred.[24,25] Given that the isotopomers of HF were dried with a pressure of F_2 prior to charging the sample can, this finding is a measure of the total [H] ingression, as H_2O is oxidized by F_2 to HF and O_2. Neutron scattering is particularly sensitive to the presence of hydrogen due to the large incoherent scattering cross-section, as discussed above.

Figure 7 shows the diffraction pattern of the sample can for DF with and without the presence of the sample for both x rays and neutrons. Whereas in Figs. 7(a) and 7(c), the presence of the sample is not immediately noticeable, in the Fourier transform of the diffraction pattern, the structure due to DF can be clearly seen overlayed with the local structure of alloy 400 [Figs. 7(b) and 7(d)]. Figure 7 shows the advantage of using a crystalline material as the material from which the cells were constructed. The background intensity is confined to the pair correlation function expected from a cubic crystalline system and subtraction of the diffraction pattern of the cell in both high energy x-ray experiments and neutron experiments proved to be tractable, though laborious, using a combination of standard methods[46,68,73] and empirical methods. The DF sample data after corrections for

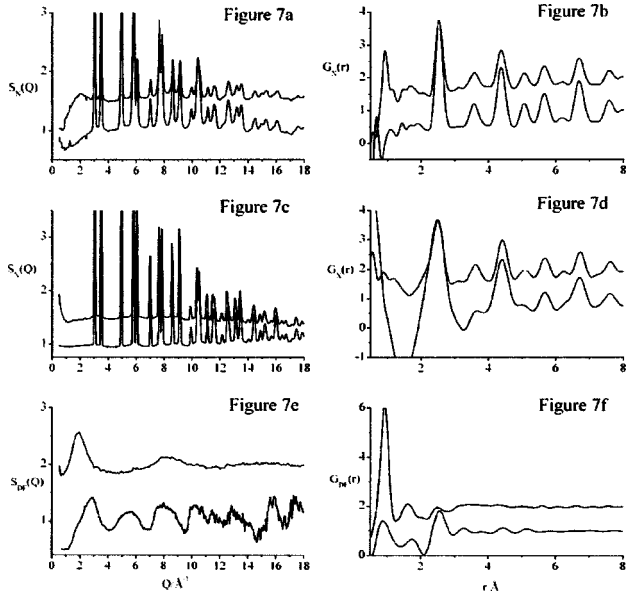

FIG. 7. (a) Neutron diffraction pattern for alloy 400, $S_N(Q)$ and for alloy 400 plus DF, $S_N(Q)+0.5$. (b) Fourier transformation of alloy 400, $G_N(r)$ and alloy 400 plus DF, $G_N(r)+1$. (c) High energy x-ray diffraction pattern for alloy 400, $S_X(Q)$ and for alloy 400 plus DF, $S_X(Q)+0.5$. (d) Fourier transformation of alloy 400, $G_X(r)$ and alloy 400 plus DF $G_X(r)+1$. (e) Corrected DF diffraction pattern using x rays, $S_{DF}(Q)$ and using neutrons $S_{DF}(Q)+1$. (f) Corrected DF Fourier transformation using x rays, $G_{DF}(r)$ and using neutrons $G_{DF}(r)+1$.

both x-ray and neutron scattering measurements are shown in Figs. 7(e) and 7(f). Previous, unpublished neutron diffraction data using PTFE cells proved to be far less tractable, with structural results that are less reliable.[74] The reason for this is clear when Fig. 1 is considered. The determination of the source of scatter from alloy 400 is far more distinct than from PTFE, both in reciprocal and real space.

Though the intensity of the background in a crystalline sample container is far more dramatic in reciprocal space than for a polymer-based cell, it is the source of the diffracted intensity that is important when considering a sample container. With a crystalline system, almost all of the background intensity, beyond that from the ubiquitous local structure, is confined to Bragg intensity, whereas for a partially or completely amorphous cell, this is not the case. The periodicity in a crystalline system, inherent due to the presence of a lattice, limits the local structure to a minimum, as in the presence of a lattice, only a small number of unique distances are required to describe the structure in real or reciprocal space.[75–78] For liquid samples, it is clear that minimization of diffuse scatter, beyond the local structure, is the most important consideration.

ACKNOWLEDGMENTS

The authors wish to extend their thanks for the provision of funding for this work to the University of Tennessee through start-up funds, the Petroleum Research Fund, administered by the American Chemical Society (PRF-37341-G4), and the Neutron Sciences Consortium of the University of Tennessee. The experiments performed at Argonne National Laboratory were supported under U.S. DOE Contract No. W-31-109-ENG-38. The authors would also like to thank Dr. J. L. Adcock (University of Tennessee) for advice and the loan of F_2/N_2 gas; B. Marzec, Dr. A. Schultz, K. Volin, M. Heinig (all of IPNS), and J. Linton and C. Kurtz (APS) for essential and material help in the facilitation of these experiments. In addition, the authors thank Dr. M. L. Klein (University of Pennsylvania) for highly stimulating discussions.

[1] D. T. Meshri, Adv. Inorg. Fluorides, 661 (2000).
[2] R. A. D. Boisson, Organofluorine Chem., 579 (1994).
[3] H. Fielding and B. Lee, Chem. Br. **14**, 173 (1978).
[4] J. Sommer, Stable Carbocation Chem., Loker Hydrocarbon Res. Inst. Symp. Carbocation Chem., 497 (1997).
[5] G. A. Olah, G. K. Surya Prakash, and J. Sommer, *Superacids* (Wiley, New York, 1985).
[6] T. A. O'Donnell, *Superacids and Acidic Melts as Inorganic Chemical Reaction Media* (VCH, New York, 1992).
[7] G. A. Olah, Angew. Chem., Int. Ed. Engl. **34**, 1393 (1995).
[8] R. J. Gillespie and J. Liang, J. Am. Chem. Soc. **110**, 6053 (1988).
[9] J. J. DeCorpo, R. P. Steiger, J. L. Franklin, and J. L. Margrave, J. Chem. Phys. **53**, 936 (1970).
[10] R. J. Le Roy and R. B. Bernstein, Chem. Phys. Lett. **5**, 42 (1970).
[11] K. P. Huber and G. Herzberg, *Molecular Spectra and Molecular Structure, 4: Constants of Diatomic Molecules* (Dover, New York, 1979).
[12] J. W. Tromp and R. J. Le Roy, J. Mol. Spectrosc. **109**, 352 (1985).
[13] B. N. Figgis and M. A. Hitchman, *Ligand Field Theory and Its Applications* (Wiley, New York, 2000).
[14] L. Graham, O. Graudejus, N. K. Jha, and N. Bartlett, Coord. Chem. Rev. **197**, 321 (2000).
[15] N. Bartlett, Proc. Chem. Soc., 218 (1962).
[16] L. Hedberg, K. Hedberg, P. G. Eller, and R. R. Ryan, Inorg. Chem. **27**, 232 (1988).
[17] R. D. Burbank and G. R. Jones, J. Am. Chem. Soc. **96**, 43 (1974).
[18] R. D. Burbank and G. R. Jones, Science **171**, 485 (1971).
[19] G. R. Jones, R. D. Burbank, and W. E. Falconer, J. Chem. Phys. **53**, 1605 (1970).
[20] R. M. Gavin, Jr. (unpublished).
[21] J. A. Ibers, J. Chem. Phys. **40**, 402 (1964).
[22] A. Pierrard, P. Gredin, and A. de Kozak, Powder Diffr. **11**, 121 (1996).
[23] S. E. McLain, C. J. Benmore, and J. F. C. Turner, J. Chem. Phys. **117**, 3816 (2002).
[24] S. E. McLain, J. J. Molaison, K. H. Herwig *et al.* (unpublished).
[25] S. E. McLain, C. J. Benmore, J. E. Siewenie, *et al.* (unpublished).
[26] E. Lalik, W. I. F. David, P. Barnes, and J. F. C. Turner, J. Phys. Chem. B **105**, 9153 (2001).
[27] J. F. C. Turner, R. Done, J. Dreyer, W. I. F. David, and C. R. A. Catlov, Rev. Sci. Instrum. **70**, 2325 (1999).
[28] J. F. C. Turner, C. J. Benmore, C. M. Barker, N. Kaltsoyannis, J. M. Thomas, W. I. F. David, and C. R. A. Catlow, J. Phys. Chem. B **104**, 7570 (2000).
[29] R. I. Walton, A. Norquist, R. I. Smith, and D. O'Hare, Faraday Discuss. **122**, 331 (2002).
[30] R. I. Walton, R. I. Smith, and D. O'Hare, Micro. and Meso. Mat. **48**, 79 (2001).
[31] R. I. Walton and D. O'Hare, Chem. Commun. (Cambridge) **23**, 2283 (2000).
[32] R. I. Walton, R. J. Francis, P. S. Halasyamani, D. O'Hare, R. I. Smith, R. Done, and R. J. Humphreys, Rev. Sci. Instrum. **70**, 3391 (1999).
[33] K. Kono *et al.*, Int. J. Occup. Environ. Health **73**, S93 (2000).
[34] J. J. Kirkpatrick, D. S. Enion, and D. A. Burd, Burns **21**, 483 (1995).
[35] ISIS Pulsed Neutron and Muon Source, Rutherford Appelton Laboratory, Chilton, Oxon, U.K., http://www.isis.rl.ac.uk
[36] W. G. Williams, R. M. Ibberson, P. Day, and E. Enderby, Physica B **241-243**, 234 (1998).
[37] General Materials Diffractometer, ISIS Pulsed Neutron and Muon Source, http://www.isis.rl.ac.uk/disordered/gem/gem_home.htm
[38] Advanced Photon Source, Argonne National Laboratory, Argonne, IL, http://www.aps.anl.gov/aps/frame_home.htm
[39] Spallation Neutron Source, Oak Ridge National Laboratory, Oak Ridge, TN, http://www.sns.gov/
[40] G. L. Squires, *Introduction to the Theory of Thermal Neutron Scattering* (Dover, New York, 1997).

[41] J. Byrne and J. M. Robson, *Neutrons, Nuclei and Matter: An Exploration of the Physics of Slow Neutrons* (Institute of Physics, University of Reading, Berkshire, 1996).
[42] Neutron News **3**, 29 (1992).
[43] NIST neutron scattering data, http:/www.ncnr.nist.gov/resources/n-lengths/
[44] R. W. James, *The Optical Principles of the Diffraction of X Rays* (Ox Bow, Woodbridge, CN, 1948).
[45] J. Neuefeind, J. Mol. Liq. **98-99**, 87 (2002).
[46] J. Neuefeind and H. F. Poulsen, Phys. Scr., T **T57**, 112 (1995).
[47] J. Neuefeind, C. J. Benmore, B. Tomberli, and P. A. Egelstaff, J. Phys.: Condens. Matter **14**, L429 (2002).
[48] T. Weitkamp, J. Neuefeind, H. E. Fischer, and M. D. Zeidle, Mol. Phys. **98**, 125 (2000).
[49] J. Neuefeind, M. D. Zeidler, and H. F. Poulsen, Mol. Phys. **87**, 189 (1996).
[50] Y. S. Badyal, M. L. Saboungi, D. L. Price, S. D. Shastri, D. Haeffne, and A. K. Soper, J. Chem. Phys. **112**, 9206 (2000).
[51] C. J. Benmore and P. A. Egelstaff, J. Phys.: Condens. Matter **8**, 9429 (1996).
[52] B. Tomberli, C. J. Benmore, P. A. Egelstaff, J. Neuefeind, and V. Honkimaki, J. Phys.: Condens. Matter **12**, 2597 (2000).
[53] B. Tomberli, C. J. Benmore, P. A. Egelstaff, J. Neuefeind, and V. Honkimaki, Europhys. Lett. **55**, 341 (2001).
[54] B. Tomberli, P. A. Egelstaff, C. J. Benmore, P. A. Egelstaff, J. Neuefeind, and V. Honkimaki, J. Phys.: Condens. Matter **13**, 11405 (2001).
[55] B. Tomberli, P. A. Egelstaff, C. J. Benmore, and J. Neuefeind, J. Phys.: Condens. Matter **13**, 11421 (2001).
[56] M. Pourbaix, *Atlas of Electrochemical Equilibria in Aqueous Solutions* (NACE International, 1966).
[57] E. Deltombe, N. de Zoubov, and M. Pourbaix, Centre Belge Etude Corrosion Technical Report No. 29 (1956), 25 pp.
[58] M. Pourbaix, Centre Belge d'Etude de la Corrosion Technical Report No. 146-7-8-9-50 (1968), 4 pp.
[59] M. Maraghini, P. van Rysselberghe, E. Deltombe, W. de Zoubov, and M. Pourbaix, Centre Belge Etude Corrosion Technical Report No. Rapp. Tech. 45 (1957), 13 pp.
[60] G. W. Stanton, J. C. Dore, and N. J. Hance, Nucl. Instrum. Methods **141**, 259 (1977).
[61] D. F. Shriver and M. A. Drezdzon, *The Manipulation of Air-Sensitive Compounds* (Wiley, New York, 1986).
[62] C. W. Bunn and E. R. Howells, Nature (London) **174**, 549 (1954).
[63] M. Sprik, U. Roethlisberger, and M. L. Klein, J. Phys. Chem. B **101**, 2745 (1997).
[64] M. Sprik, U. Rothlisberger, and M. L. Klein, Mol. Phys. **97**, 355 (1999).
[65] E. Dobnik and W. Borchard, Makromol. Chem., Macromol. Symp. **39**, 249 (1990).
[66] I. V. Sysoev and V. S. Khanarin, Zh. Fiz. Khim. **58**, 735 (1984).
[67] GLAD homepage, http://www.pns.anl.gov/glad/glad.htm
[68] A. K. Soper, W. S. Howells, and A. C. Hannon, *ATLAS Manual* (ISIS Pulsed Neutron Source, Rutherford Appleton Laboratory, 1989).
[69] A. K. Soper, Nucl. Instrum. Methods Phys. Res. **212**, 337 (1983).
[70] H. F. Poulsen, J. Neuefeind, H. B. Neumann, J. R. Schneider, and M. D. Zeidler, J. Non-Cryst. Solids **188**, 63 (1995).
[71] A. K. Soper and P. A. Egelstaff, Nucl. Instrum. Methods **178**, 415 (1980).
[72] K. F. Bradley, S. H. Chen, T. O. Brun, R. Kleb, W. A. Looinis, and J. M. Newsam, Nucl. Instrum. Methods Phys. Res. A **270**, 78 (1988).
[73] J. Urquidi, C. J. Benmore, J. Neuefeind, and B. Tomberli, J. Appl. Crystallogr. **36**, 368 (2003).
[74] S. E. McLain, C. J. Benmore, J. Urquidi, and J. F. C. Turner (unpublished results).
[75] D. L. Goodstein, *States of Matter* (Dover, Mineola, NY, 2002).
[76] W. H. Zachariasen, *Theory of X-Ray Diffraction in Crystals* (Dover, New York, 1995).
[77] A. Guinier, *X-Ray Diffraction in Crystals, Imperfect Crystals, and Amorphous Bodies* (Dover, New York, 1963).
[78] N. H. March and M. P. Tosi, *Atomic Dynamics in Liquids* (1976).